Numerical simulation and stability analysis for the fractional-order dynamics of COVID-19

Harendra Singh [a], H.M. Srivastava [b,c,d], Zakia Hammouch [e], Kottakkaran Sooppy Nisar [f,*]

[a] Department of Mathematics, Post-Graduate College, Ghazipur 233001, Uttar Pradesh, India
[b] Department of Mathematics and Statistics, University of Victoria, British Columbia V8W 3R4, Canada
[c] Department of Medical Research, China Medical University Hospital, China Medical University, Taichung 40402, Taiwan
[d] Department of Mathematics and Informatics, Azerbaijan University, 71 Jeyhun Hajibeyli Street, AZ1007 Baku, Azerbaijan
[e] Division of Applied Mathematics, Thu Dau Mot University, Binh Duong Province, Vietnam
[f] Department of Mathematics, College of Arts and Sciences, Prince Sattam Bin Abdulaziz University, 11991 Wadi Aldawasir, Saudi Arabia

ABSTRACT

The main purpose of this work is to study the dynamics of a fractional-order Covid-19 model. An efficient computational method, which is based on the discretization of the domain and memory principle, is proposed to solve this fractional-order corona model numerically and the stability of the proposed method is also discussed. Efficiency of the proposed method is shown by listing the CPU time. It is shown that this method will work also for long-time behaviour. Numerical results and illustrative graphical simulation are given. The proposed discretization technique involves low computational cost.

Introduction

In the year 2020, the corona virus pandemic has become one of the major problems worldwide. This virus produces lung infection and is highly spread from human to human [1]. Due to the effect of the corona virus on human body, many causalities in the world are caused. The first case of the corona virus was officially reported in the city of Wuhan in the People's Republic of China on December 31, 2019 (see [2]). The available treatments and vaccines were not effective for this type of virus [3]. Initially this virus started to spread into the other cities of the People's Republic of China and then to other regions of the world such as Europe, Asia Pacific, North America, and so on. It has now spread in as many as 175 countries. It is recognized that the presence of the symptoms takes 2 to 10 days. The symptoms include the breathing difficulties, coughing and high fever. As per reports dated March 22, 2020, around the world 250,000 cases were found to be infected with the virus and there were 15,000 deaths.

Aiming to propose a suitable dynamical system for the evolution of the pandemic spreading, in the following we propose a fractional-order dynamical model for the analysis of the virus spread, thereby showing that our model is best fitting with the available observations. Fractional calculus [4–14] has many real life applications. Here, we propose a

scheme for solving the fractional-order corona virus model as suggested by Khan and Atangana [15] who presented the mathematical results of the model and then formulated a fractional-order model by using the Atangana-Baleanu fractional derivative. They considered the available infection cases for the period from January 21, 2020 to January 28, 2020 and parameterized the model. Using iterative technique, some concluding remarks were also given in [15]. In [16 and 17], authors modelled the transmission dynamics of COVID-19 and also solved these models numerically. In recent years a lot of numerical and analytical techniques are proposed to solve biological models [18–26].

This paper is organized as follows. In Section 2, some preliminary remarks on the Khan-Atangana model are given. Further, in Section 3, some remarks on the Grünwald-Leitnikov fractional derivative are given. Section 4 deals with the iterative scheme for the fractional-order corona virus model. In Section 5, the stability of the proposed model is discussed for our considered parameters. Section 6 deals with the numerical simulation of our results. Lastly, in Section 7, some concluding remarks and observations are given.

The Khan-Atangana model for virus spread

In the Khan-Atangana paper [15], it is assumed that the $N(t)$ denoted

* Corresponding author.
  E-mail addresses: harendra059@gmail.com (H. Singh), harimsri@math.uvic.ca (H.M. Srivastava), hammouch_zakia@tdmu.edu.vn (Z. Hammouch), n.sooppy@psau.edu.sa (K. Sooppy Nisar).

total population at time t might be divided into five subgroups as follows:

$A(t)$ is susceptible people subgroup; $B(t)$ is the exposed people subgroup; $C(t)$ is the infected people subgroup; $D(t)$ is the subgroup of asymptotically people that is people showing no symptoms of the infection and $E(t)$ is the subgroup of recovered or removed people. These are specified by $N(t) = A(t) + B(t) + C(t) + D(t) + E(t)$. So that we have the following set of nonlinear equations:

$$\frac{dA(t)}{dt} = \mu_1 - a_1 A - \frac{b_1 A(C + \sigma D)}{N} - b_2 AF$$

$$\frac{dB(t)}{dt} = \frac{b_1 A(C + \sigma D)}{N} + b_2 AF - (1-d)f_1 B - de_1 B - a_1 B$$

$$\frac{dC(t)}{dt} = (1-d)f_1 B - (g_1 + a_1)C$$

$$\frac{dD(t)}{dt} = de_1 B - (g_2 + a_1)D$$

$$\frac{dE(t)}{dt} = g_1 C + g_2 D - a_1 E$$

$$\frac{dF(t)}{dt} = a_2 \frac{FC_h}{N_h} + e_2 C + f_2 D - \mu_2 F \qquad (1)$$

In this model, μ_1 is the natural birth rate, a_1 represents the natural death rate. The susceptible people A and the infected people C are related by $b_1 AC$, where b_1 is the disease spread coefficient by which the susceptible people are infected by sufficient number of contacts. The susceptible people A and the people showing no symptoms of the infection D are related by $\sigma b_1 AD$, where $\sigma \in [0,1]$ is the transmissibility multiple of D to C. The parameter d is the proportion of the asymptomatic infection, the parameter f_1 is the spread rate after completing the incubation period and becomes infected and e_1 is spread rate joining the classes C and D. The people in the classes C and D are related to the people in the class E by recovery or removal rate g_1 and g_2 respectively. The class F denote the reservoir (outbreak of infection) or the seafood market or place. The people in the class A are related to the people in the class F by disease spread coefficient b_2. The parameter a_2 denote the host visiting the seafood market by purchasing the items. The classes C and D contribute the virus into the seafood market F by the rate e_2 and f_2, respectively. The parameter μ_2 is the removing rate of the virus from the seafood market F. N_h and I_h denote the unknown and infected hosts, respectively. Ignoring of the contact between bats and hosts, then the model (1) becomes as follows (see [15]):

$$\frac{dA(t)}{dt} = \mu_1 - a_1 A - \frac{b_1 A(C + \sigma D)}{N} - b_2 AF$$

$$\frac{dB(t)}{dt} = \frac{b_1 A(C + \sigma D)}{N} + b_2 AF - (1-d)f_1 B - de_1 B - a_1 B$$

$$\frac{dC(t)}{dt} = (1-d)f_1 B - (g_1 + a_1)C$$

$$\frac{dD(t)}{dt} = de_1 B - (g_2 + a_1)D$$

$$\frac{dE(t)}{dt} = g_1 C + g_2 D - a_1 E$$

$$\frac{dF(t)}{dt} = e_2 C + f_2 D - \mu_2 F \qquad (2)$$

The corona virus model depends on the initial conditions and the integer-order corona virus model cannot explain perfectly the virus spread due to the local nature of the integer-order derivative. The fractional derivatives are non-local in nature and depend on the initial

conditions. Therefore, for better understanding of the corona virus model, it is required to replace the integer-order corona virus model to the fractional-order model. In the following investigation, we will replace time-derivative in model (2) with the fractional-order time-derivative. We thus propose study the covid-19 infection by this original fractional-order model, based on the Khan-Atangana system (1):

$$aD_t^{p_1} A(t) = \mu_1 - a_1 A - \frac{b_1 A(C + \sigma D)}{N} - b_2 AF$$

$$aD_t^{p_2} B(t) = \frac{b_1 A(C + \sigma D)}{N} + b_2 AF - (1-d)f_1 B - de_1 B - a_1 B$$

$$aD_t^{p_3} C(t) = (1-d)f_1 B - (g_1 + a_1)C$$

$$aD_t^{p_4} D(t) = de_1 B - (g_2 + a_1)D$$

$$aD_t^{p_5} E(t) = g_1 C + g_2 D - a_1 E$$

$$aD_t^{p_6} F(t) = e_2 C + f_2 D - \mu_2 F \qquad (3)$$

The initial conditions are given below:

$$A(0) = d_1, B(0) = d_2, C(0) = d_3, D(0) = d_4, E(0) = d_5 \text{ and } F(0) = d_6, \qquad (4)$$

where $0 \leq p_1, p_2, p_3, p_4, p_5, p_6 < 1$. The additional parameters of the fractional derivatives, that is, $p_1, p_2, \cdots, p_6$ give us some extra degrees of freedom for a better approximation of the experimental data.

Some remarks on the Grünwald-Leitnikov derivative

In the present section, some basic definitions of fractional GL derivative and concept of stability analysis will be discussed first. These basic concepts are very important for understanding the fractional-order model and its stability.

Definition. ((*see* [27])) *The Grünwald–Letnikov derivative at a point a is given as follows*:

$$aD_t^p g(t) = \lim_{h \to 0} \frac{1}{h^p} \sum_{j=0}^{[n]} (-1)^j \binom{p}{j} g(t - jh) \qquad (5)$$

where $n = \frac{t-a}{h}$ and a is a real constant.

The general fractional-order linear system can be considered as follows:

$$aD_t^p x(t) = Ax(t) + Bu(t) \qquad (6)$$

Using the definition of fractional GL derivative as given in Eq. (5), at the points $kh(k = 1, 2, \cdots)$ the $p-th$ order Grünwald–Letnikov derivative has the following form

$$(k - L/h)D_{t_k}^p g(t) \approx h^{-p} \sum_{j=0}^{k} (-1)^j \binom{p}{j} g(t_{k-j}) \qquad (7)$$

where the "memory length" is L, $t_k = kh$, h is the step size taken for the calculation and the coefficients of the derivative $c_j^{(p)}(j = 0, 1, \cdots)$ and can be obtained by taking the following expressions

$$c_0^{(p)} = 1 \text{ and } c_j^{(p)} = \left(1 - \frac{1+p}{j}\right) c_{j-1}^{(p)} \qquad (8)$$

Further, using this the general from solution of the equation

$$aD_t^p y(t) = g(y(t), t) \qquad (9)$$

can be written as

$$y(t_k) = g(y(t_k), t_k) h^p - \sum_{j=v}^{k} c_j^{(p)} y(t_{k-j}) \qquad (10)$$

We will use short memory principle to determine the lower index in the sum. By the use of short memory principle the lower index is considered as

$$v = \begin{cases} 1, k < (L/h) \\ k - (L/h), k > (L/h) \end{cases} \tag{11}$$

The L can be calculated using the $L \geq \left(\frac{M}{\varepsilon |\Gamma.(1-p)|} \right)^{1/p}$.

The general fractional-order systems can be considered as

$$aD_t^q x_i(t) = f_i(x_1, x_2, \cdots, x_i, .., x_n), i = 1, 2, \cdots.n, \tag{12}$$

where aD_t^q is fractional GL derivative and $q \in (0, 1]$. For the system (12), the equilibrium is obtained by solving

$$aD_t^q x_i(t) = 0, i = 1, 2, \cdots.n \tag{13}$$

For system (12), the Jacobian matrix is written by

$$\begin{bmatrix} \frac{\partial f_1}{\partial x_1} & \cdots & \frac{\partial f_1}{\partial x_n} \\ \vdots & \ddots & \vdots \\ \frac{\partial f_n}{\partial x_1} & \cdots & \frac{\partial f_n}{\partial x_n} \end{bmatrix}$$

The Jacobian matrix at equilibrium point $(b_1, b_2, \cdots, b_n)$ is given by:

$$\begin{bmatrix} \frac{\partial f_1}{\partial x_1} & \cdots & \frac{\partial f_1}{\partial x_n} \\ \vdots & \ddots & \vdots \\ \frac{\partial f_n}{\partial x_1} & \cdots & \frac{\partial f_n}{\partial x_n} \end{bmatrix}_{(b_1, b_2, \cdots, b_n)} \tag{15}$$

Theorem 1. (*[28,29].*)   *If all the eigenvalues of matrix given in Eq. (15), satisfied the condition*

$$|\arg(\lambda)| > \frac{p_i \pi}{2}, \text{where} i = 1, 2, 3, 4, 5, 6 \tag{16}$$

Then system given in (12), is locally stable.

The numerical solution of the Khan-Atangana model

In this section we will implement our proposed technique to solve the corona virus model. The integer order corona virus model which is specified as

$$\frac{dA(t)}{dt} = \mu_1 - a_1 A - \frac{b_1 A(C + \sigma D)}{N} - b_2 AF$$

$$\frac{dB(t)}{dt} = \frac{b_1 A(C + \sigma D)}{N} + b_2 AF - (1 - d)f_1 B - de_1 B - a_1 B$$

$$\frac{dC(t)}{dt} = (1 - d)f_1 B - (g_1 + a_1)C$$

$$\frac{dD(t)}{dt} = de_1 B - (g_2 + a_1)D$$

$$\frac{dE(t)}{dt} = g_1 C + g_2 D - a_1 E$$

$$\frac{dF(t)}{dt} = e_2 C + f_2 D - \mu_2 F \tag{17}$$

Integrating both sides of Eq. (17), we have

$$A(t) = \int_0^t \left[\mu_1 - a_1 A - \frac{b_1 A(C + \sigma D)}{N} - b_2 AF \right] dt$$

$$B(t) = \int_0^t \left[\frac{b_1 A(C + \sigma D)}{N} + b_2 AF - (1 - d)f_1 B - de_1 B - a_1 B \right] dt$$

$$C(t) = \int_0^t [(1 - d)f_1 B - (g_1 + a_1)C] dt$$

$$D(t) = \int_0^t [de_1 B - (g_2 + a_1)D] dt$$

$$E(t) = \int_0^t [g_1 C + g_2 D - a_1 E] dt$$

$$F(t) = \int_0^t [e_2 C + f_2 D - \mu_2 F] dt \tag{18}$$

The fractional-order corona model using GL derivative is given as

$$aD_t^{p_1} A(t) = \mu_1 - a_1 A - \frac{b_1 A(C + \sigma D)}{N} - b_2 AF$$

$$aD_t^{p_2} B(t) = \frac{b_1 A(C + \sigma D)}{N} + b_2 AF - (1 - d)f_1 B - de_1 B - a_1 B$$

$$aD_t^{p_3} C(t) = (1 - d)f_1 B - (g_1 + a_1)C$$

$$aD_t^{p_4} D(t) = de_1 B - (g_2 + a_1)D$$

$$aD_t^{p_5} E(t) = g_1 C + g_2 D - a_1 E$$

$$aD_t^{p_6} F(t) = e_2 C + f_2 D - \mu_2 F \tag{19}$$

Taking the fractional integral on both sides of Eq. (19) and using Eq. (18), we have

$$A(t) = aD_t^{1-p_1} \left(\int_0^t \left[\mu_1 - a_1 A - \frac{b_1 A(C + \sigma D)}{N} - b_2 AF \right] dt \right)$$

$$B(t) = aD_t^{1-p_2} \left(\int_0^t \left[\frac{b_1 A(C + \sigma D)}{N} + b_2 AF - (1 - d)f_1 B - de_1 B - a_1 B \right] dt \right)$$

$$C(t) = aD_t^{1-p_3} \left(\int_0^t [(1 - d)f_1 B - (g_1 + a_1)C] dt \right)$$

$$D(t) = aD_t^{1-p_4} \left(\int_0^t [de_1 B - (g_2 + a_1)D] dt \right)$$

$$E(t) = aD_t^{1-p_5} \left(\int_0^t [g_1 C + g_2 D - a_1 E] dt \right)$$

$$F(t) = aD_t^{1-p_6} \left(\int_0^t [e_2 C + f_2 D - \mu_2 F] dt \right) \tag{20}$$

By using the fractional GL derivative definition in Eq. (20), we obtain the following relations

$$A(t_k) = \left(\mu_1 - a_1 A(t_{k-j}) - \frac{b_1 A(t_{k-j})(C(t_{k-j}) + \sigma D(t_{k-j}))}{N} - b_2 A(t_{k-j}) F(t_{k-j})\right) h^{p_1}$$
$$- \sum_{j=v}^{k} c_j^{(p_1)} A(t_{k-j})$$

$$B(t_k) = \left(\frac{b_1 A(t_k)(C(t_{k-j}) + \sigma D(t_{k-j}))}{N} + b_2 A(t_k) F(t_{k-j}) - (1$$
$$- d) f_1 B(t_{k-j}) - d e_1 B(t_{k-j}) - a_1 B(t_{k-j})\right) h^{p_2} - \sum_{j=v}^{k} c_j^{(p_2)} B(t_{k-j})$$

$$C(t_k) = \left((1 - d) f_1 B(t_k) - (g_1 + a_1) C(t_{k-j})\right) h^{p_3} - \sum_{j=v}^{k} c_j^{(p_3)} C(t_{k-j})$$

$$D(t_k) = \left(d e_1 B(t_k) - (g_2 + a_1) D(t_{k-j})\right) h^{p_4} - \sum_{j=v}^{k} c_j^{(p_4)} D(t_{k-j})$$

$$E(t_k) = \left(g_1 C(t_k) + g_2 D(t_k) - a_1 E(t_{k-j})\right) h^{p_5} - \sum_{j=v}^{k} c_j^{(p_5)} E(t_{k-j})$$

$$F(t_k) = \left(e_2 C(t_k) + f_2 D(t_k) - \mu_2 F(t_{k-j})\right) h^{p_6} - \sum_{j=v}^{k} c_j^{(p_6)} F(t_{k-j}) \quad (21)$$

Further, solving Eq. (21), we will get unknowns in fractional corona virus model. Now desired accuracy can be obtained by iterating Eq. (21). For the better accuracy of solution the step size will be minimized. The minimization in step size will increase the number of iterations as a result the computation time will be increased. For the numerical simulation of our results we have considered step-size $h = 0.01$.

Stability analysis

Here, we discuss the stability of this epidemiological model. The equilibrium points for system (19) is given by

$$aD_t^{p_1} A(t) = \mu_1 - a_1 A - \frac{b_1 A(C + \sigma D)}{N} - b_2 A F = 0$$

$$aD_t^{p_2} B(t) = \frac{b_1 A(C + \sigma D)}{N} + b_2 A F - (1 - d) f_1 B - d e_1 B - a_1 B = 0$$

$$aD_t^{p_3} C(t) = (1 - d) f_1 B - (g_1 + a_1) C = 0$$

$$aD_t^{p_4} D(t) = d e_1 B - (g_2 + a_1) D = 0$$

$$aD_t^{p_5} E(t) = g_1 C + g_2 D - a_1 E = 0$$

$$aD_t^{p_6} F(t) = e_2 C + f_2 D - \mu_2 F = 0 \quad (22)$$

For the above system the Jacobian matrix is defined as:

For this model we will calculate disease-free equilibrium points as well as the endemic- equilibrium points. The disease-free and endemic-equilibrium points are characterized by the non-existence and existence of the infected nodes, respectively. With the values $= 8,266,000$ $\mu_1 = 107644.22451$, $\mu_2 = 0.01$, $a_1 = \frac{1}{76.79}$, $b_1 = 0.05$, $b_2 = 0.000001231$, $\sigma = 0.02$, $d = 0.1243$, $f_1 = 0.00047876$, $f_2 = 0.001$, $e_1 = 0.005$, $e_2 = 0.000398$, $g_1 = 0.09871$, $g_2 = 0.854302$ the disease-free equilibrium point is given as $\left(\frac{\mu_1}{a_1}, 0, 0, 0, 0, 0\right)$, and the endemic- equilibrium points are given as $(4.76 \times 10^7, -3.65 \times 10^7, -1.37 \times 10^5, -2.61 \times 10^4, -2.75 \times 10^6, -8.07 \times 10^3)$.

The Jacobian matrix at disease-free equilibrium point $\left(\frac{\mu_1}{a_1}, 0, 0, 0, 0, 0\right)$ is given as follows:

$$J_1 = \begin{bmatrix} -0.0130 & 0 & -0.0500 & -0.0010 & 0 & -10.1754 \\ 0 & -0.0141 & 0.0500 & 0.0010 & 0 & 10.1754 \\ 0 & 0.0004 & -0.1117 & 0 & 0 & 0 \\ 0 & 0.0006 & 0 & -0.8673 & 0 & 0 \\ 0 & 0 & 0.0987 & 0.8543 & -0.0130 & 0 \\ 0 & 0 & 0.0003 & 0.0010 & 0 & -0.0100 \end{bmatrix}$$
$$(23)$$

The eigenvalues corresponding to matrix J_1 are $\lambda_1 = -0.0130$, $\lambda_2 = -0.0130$, $\lambda_3 = -0.1118$, $\lambda_4 = -0.0067$, $\lambda_5 = -0.0173$ and $\lambda_6 = -0.8673$. J_1 has negative eigenvalues. Therefore, by definition, the system (19) is stable for $0 < p_i < 1$, $i = 1, 2, 3, 4, 5, 6$ at the equilibrium point $\left(\frac{\mu_1}{a_1}, 0, 0, 0, 0, 0\right)$. The Jacobian matrix at the endemic-equilibrium point $(4.76 \times 10^7, -3.65 \times 10^7, -1.37 \times 10^5, -2.61 \times 10^4, -2.75 \times 10^6, -8.07 \times 10^3)$ is given as follows:

$$J_2 = \begin{bmatrix} -0.0023 & 0 & -0.2885 & -0.0058 & 0 & -58.7180 \\ -0.0108 & -0.0141 & 0.2885 & 0.0058 & 0 & 58.7180 \\ 0 & 0.0004 & -0.1117 & 0 & 0 & 0 \\ 0 & 0.0006 & 0 & -0.8673 & 0 & 0 \\ 0 & 0 & 0.0987 & 0.8543 & -0.0130 & 0 \\ 0 & 0 & 0.0003 & 0.0010 & 0 & -0.0100 \end{bmatrix}$$
$$(24)$$

The eigenvalues corresponding to the matrix J_2 are $\lambda_1 = -0.0130$, $\lambda_2 = -0.8673$, $\lambda_3 = -0.1120$, $\lambda_4 = -0.0195$, $\lambda_5 = -0.0127$ and $\lambda_6 = 0.0061$. By definition, the system (19) is asymptotically unstable at the endemic-equilibrium point $(4.76 \times 10^7, -3.65 \times 10^7, -1.37 \times 10^5, -2.61 \times 10^4,$
$$-2.75 \times 10^6, -8.07 \times 10^3)$$

. Since it has five negative eigenvalues, therefore it has five dimensional stable manifolds. So, by a physical point of view, we can draw its three dimensional manifolds.

$$J = \begin{bmatrix} -a_1 - \frac{b_1(C + \sigma D)}{N} - b_2 F & 0 & -\frac{b_1 A}{N} & -\frac{b_1 \sigma A}{N} & 0 & -b_2 A \\ \frac{b_1(C + \sigma D)}{N} + b_2 F & -(1 - d) f_1 - d e_1 - a_1 & \frac{b_1 A}{N} & \frac{b_1 \sigma A}{N} & 0 & b_2 A \\ 0 & (1 - d) f_1 & -(g_1 + a_1) & 0 & 0 & 0 \\ 0 & d e_1 & 0 & -(g_2 + a_1) & 0 & 0 \\ 0 & 0 & g_1 & g_2 & -a_1 & 0 \\ 0 & 0 & e_2 & f_2 & 0 & -\mu_2 \end{bmatrix}$$

Results and discussion

In this section we present numerical results assuming the initial conditions $A(0) = 8065518$, $B(0) = 200000$, $C(0) = 282$, $D(0) = 200$, $E(0) = 0$ and $F(0) = 50000$. Fig. 1, shows the behaviour of group of (A) with time. From Fig. 1, it can be seen that susceptible people group decreases and tends to zero. Fig. 2, shows exposed group (B) with respect to time. From Fig. 2, it can be seen that exposed people increases with time. Fig. 3, shows the group of infected or symptomatic people (C) with respect to time. From Fig. 3, it can be seen that initially it increases, but after some time it start to decrease, that is, people are recovered after treatment. Fig. 4, shows asymptotically infected group (D) with respect to time. From Fig. 4, it can been seen that it increases with time. Fig. 5, shows the group of people who are recovered or remove (E) with respect to time. From Fig. 5, it can be seen that it increases with time showing the accuracy and applicability of the proposed model. Fig. 6 shows performance of reservoir group (E) with time. From Fig. 6, it can be seen that it decreases, that is, reservoir after some time become negligible.

Fig. 7 displays the dynamics of $A(t)$, $B(t)$ and $C(t)$ for integer-order time-derivative. Fig. 7 shows the 3D trajectory for the group of $A(t)$, $B(t)$ and $C(t)$ at integer-order time-derivative and starting at
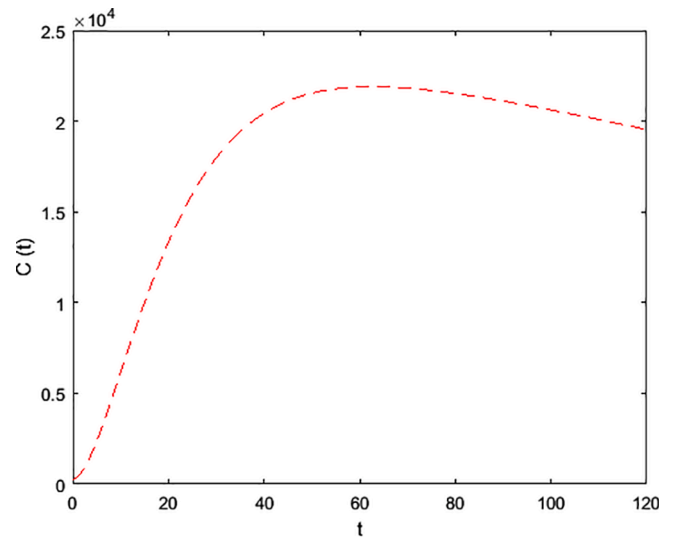

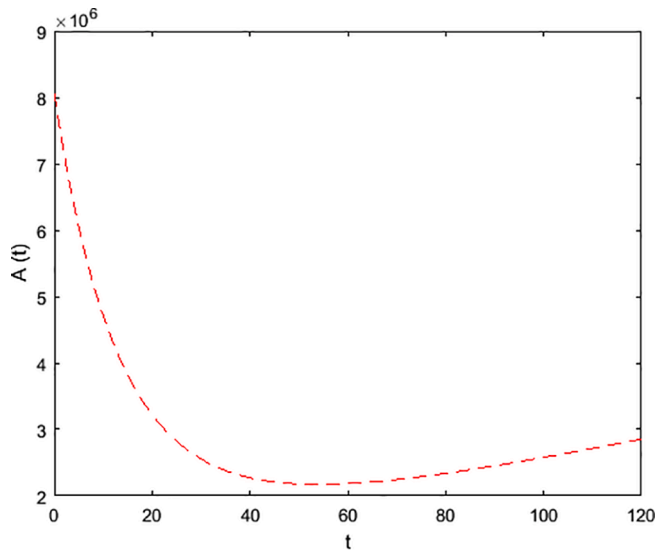**Fig. 3.** Performance of group (C) with time.
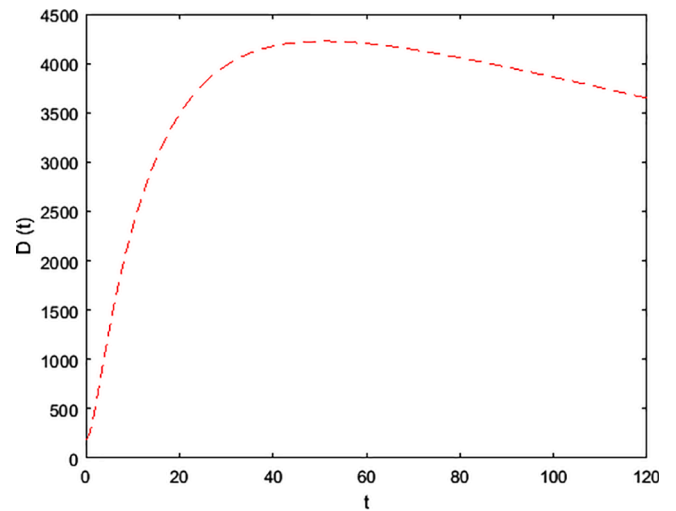

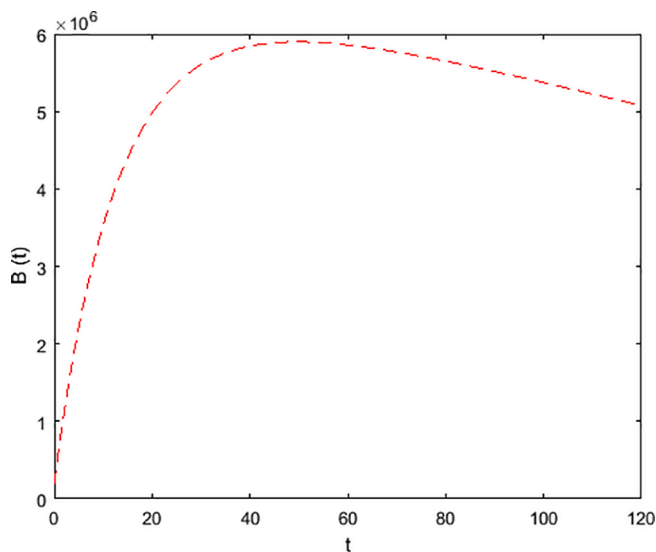**Fig. 1.** Performance of group (A) with time.

Fig. 4. Performance of group (D) with time.
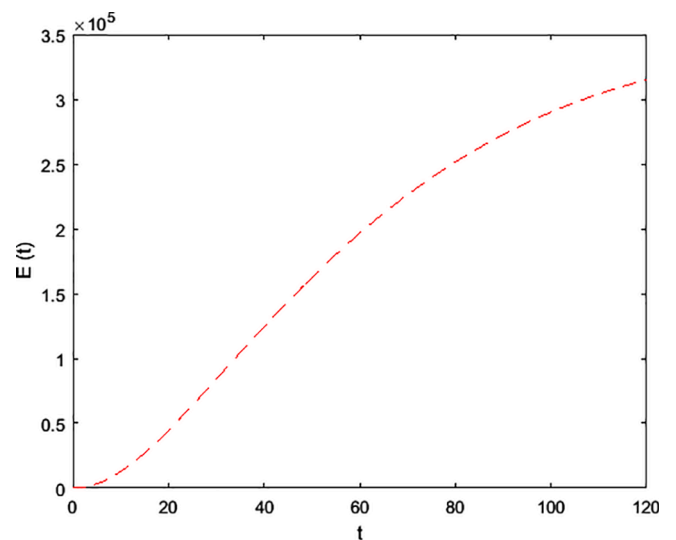

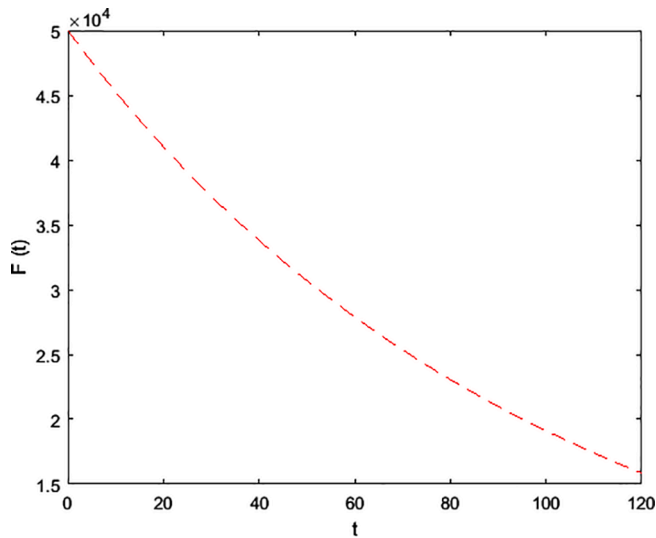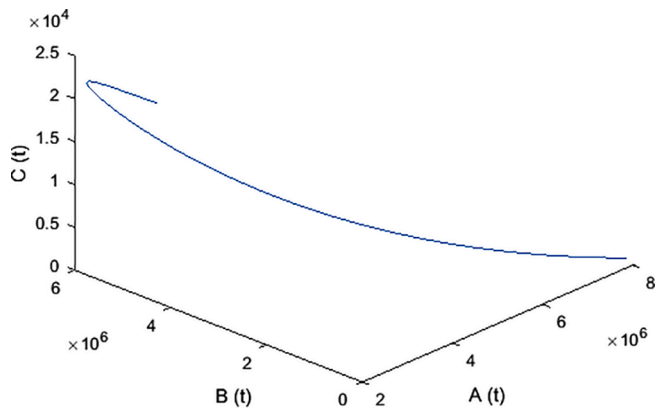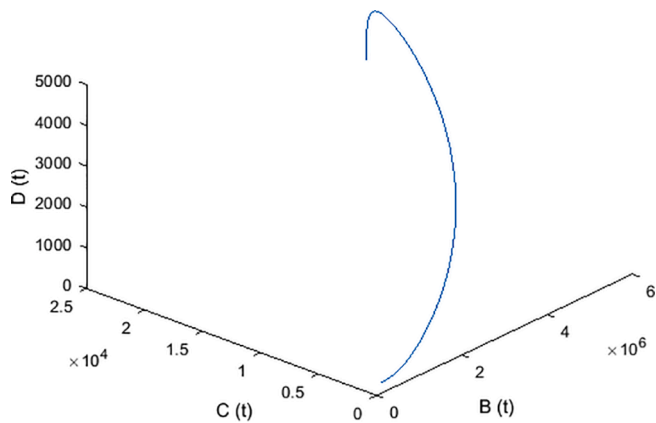**Fig. 2.** Performance of group (B) with time.
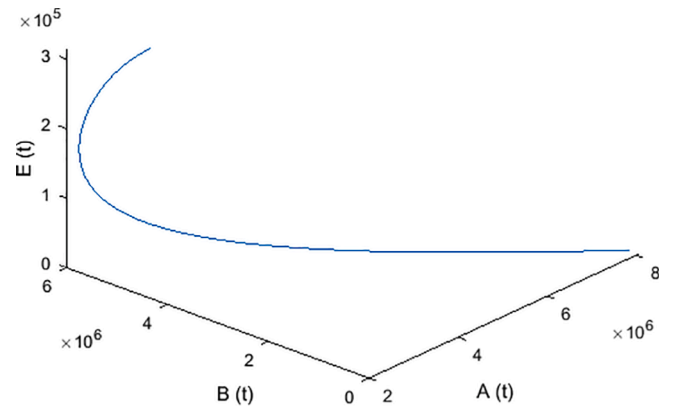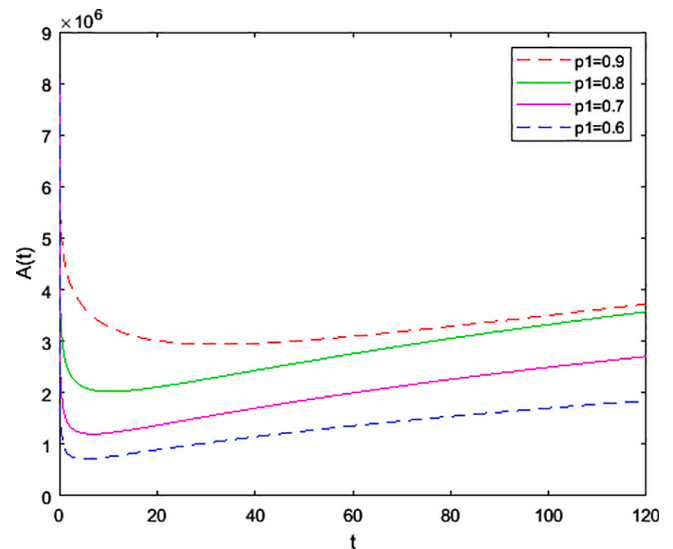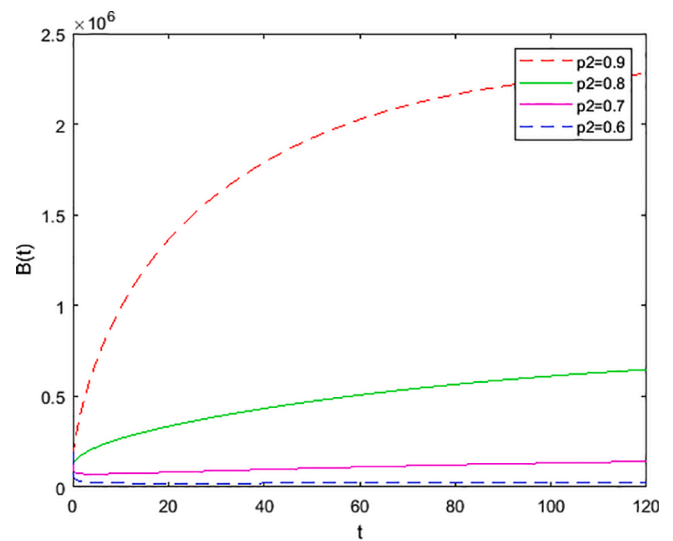

Fig. 5. Performance of group (E) with time.

Fig. 6. Performance of group (F) with time.

Fig. 7. Performance of groups $A(t)$, $B(t)$ and $C(t)$ for integer order relaxation.

Fig. 8. Performance of groups $B(t)$, $C(t)$ and $D(t)$ for integer order relaxation.

Fig. 9. Performance of groups $A(t)$, $B(t)$ and $E(t)$ for integer order relaxation.

Fig. 10. Performance of group $A(t)$ with time at distinct fractional values of time-derivatives.

Fig. 11. Performance of group $B(t)$ with time at distinct fractional values of time-derivatives.

$(A(0) = 8065518, B(0) = 200000, C(0) = 282)$. Fig. 8 displays the dynamics of the exposed people $B(t)$, the symptomatic people $C(t)$ and the asymptomatically infected people $D(t)$ for integer-order time-derivative. Fig. 8 shows the 3D trajectory for the group of the exposed people $B(t)$, the symptomatic people $C(t)$ and the asymptomatically infected people $D(t)$ at integer-order time-derivative and starting at $(B(0) = 200000, C(0) = 282, D(0) = 200)$. Fig. 9 displays the dynamics

Fig. 12. Performance of group $C(t)$ with time at distinct fractional values of time-derivatives.
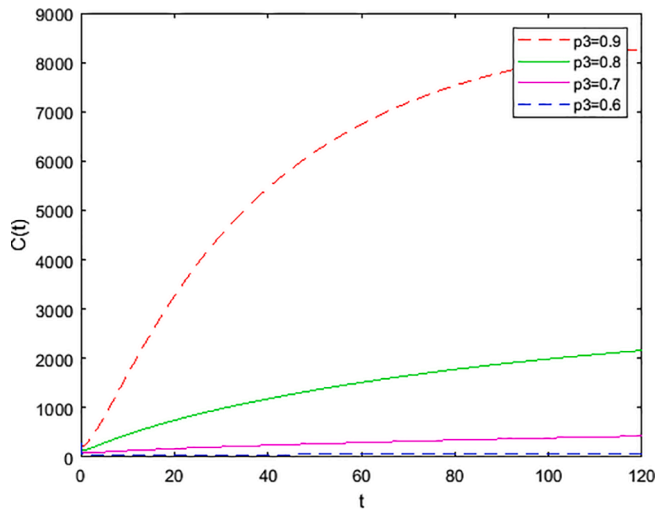

Fig. 14. Performance of group $E(t)$ with time at distinct fractional values of time-derivatives.

of the susceptible people $A(t)$, the exposed people $B(t)$ and the removed or recovered people $E(t)$ for integer-order time-derivative. Fig. 9 shows the 3D trajectory for the group of the susceptible people $A(t)$, the exposed people $B(t)$ and the recovered people $E(t)$ at integer-order time-derivative and starting at $(A(0) = 8065518, B(0) = 200000, E(0) = 0)$.

In Fig. 10, we have shown the dynamical performance of the group $A(t)$ with time by taking distinct fractional values of time-derivatives. From Fig. 10, it can be seen that a continuous variations for the group of the susceptible people $A(t)$ take place depending upon the values of the involved parameters and the values of the order of the fractional derivatives. The group $A(t)$ shows monotonic behaviour with the fractional-order time-derivative. In Fig. 11, we have shown the dynamical performance of $B(t)$ with time by taking distinct fractional values of time-derivatives. From Fig. 11, it can be seen that a continuous variation for the group of the exposed people $B(t)$ takes place depending upon the values of the involved parameters and the values of the order of the fractional derivatives. The group of the exposed people $B(t)$ shows monotonic behaviour with the fractional-order time-derivative. In Fig. 12, we have shown the dynamical performance of the group $C(t)$ with time by taking distinct fractional values of time-derivatives. From Fig. 12, it can be seen that a continuous variation for the group of group of the symptomatic people $C(t)$ takes place depending upon the values of
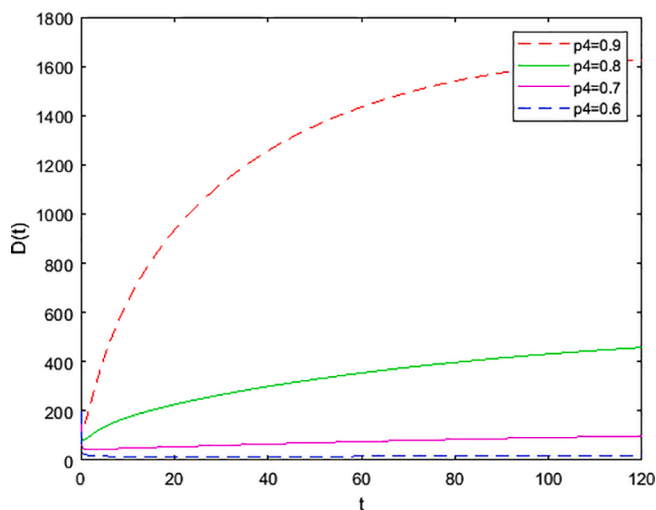
the involved parameters and the values of the order of the fractional derivatives. $C(t)$ shows monotonic behaviour with the fractional-order time-derivative. In Fig. 13, we have shown the dynamical performance of the group $D(t)$ with time by taking distinct fractional values of time-derivatives. From Fig. 13, it can be seen that a continuous variation for $D(t)$ takes place depending upon the values of the involved parameters and the values of the order of the fractional derivatives. The asymptomatically infected people group $D(t)$ shows monotonic behaviour with the fractional-order time-derivative. In Fig. 14, we have shown the dynamical performance of the group $E(t)$ with time by taking distinct fractional values of time-derivatives. From Fig. 14, it can be seen that a continuous variation for the group of people who are recovered $E(t)$ takes place depending upon the values of the involved parameters and the values of the order of the fractional derivatives. The group of people who are recovered $E(t)$ shows monotonic behaviour with the fractional-order time-derivative. In Fig. 15, we have shown the dynamical performance of $F(t)$ with time by taking distinct fractional values of time-derivatives. From Fig. 15, it can be seen that a continuous variation for the group of reservoir $F(t)$ takes place depending upon the values of

Fig. 13. Performance of group $D(t)$ with time at distinct fractional values of time-derivatives.
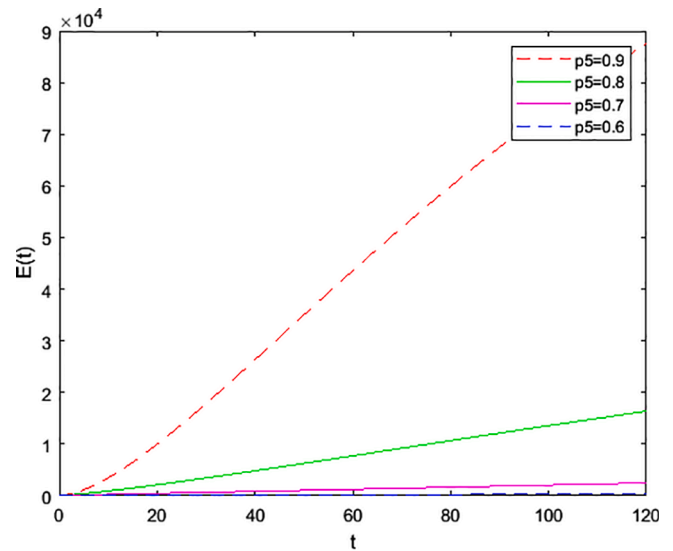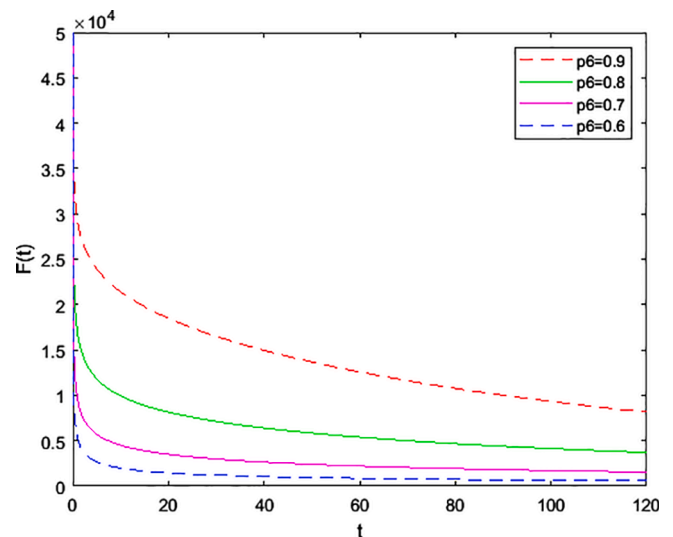

Fig. 15. Performance of group $F(t)$ with time at distinct fractional values of time-derivatives.

Table 1
CPU time of computation.

Δt	n	Time (s)
0.1	1200	0.478
0.01	12,000	37.709
0.2	600	0.524
0.02	6000	12.124

the involved parameters and the values of the order of the fractional derivatives. The group of reservoir $F(t)$ shows monotonic behaviour with the fractional-order time-derivative.

In Table 1, we have listed the CPU time taken in the computation of the numerical results by our proposed technique. From this table, the efficiency of the proposed technique is clear. It is also clear that the technique is time-saving.

Conclusions

In this paper a computational method, which is based on the discretization of the domain and short memory principle, is implemented to solve a fractional-order corona virus model numerically. The proposed algorithm is attractive and time-saving as can be seen from Table 1. The figures in this paper show that the solution varies continuously depending on fractional derivatives and on the values of parameters. From numerical and stability discussion, it can be seen that, at a time t, the fractional-order corona virus model depends on its parameters. Therefore, the values of these parameters play a key role to increase the number of the recovered people and decrease the number of the infected people. The proposed technique is effective to show the behaviour of the solution in a very long time-period which is helpful to predict the corona virus model accurately. This method can be used in investigating many similar biological models showing wide applicability of the proposed method.

Funding

None.

CRediT authorship contribution statement

Harendra Singh: Conceptualization, Writing - original draft, Software. **H.M. Srivastava:** Conceptualization, Writing - original draft, Formal analysis, Methodology. **Zakia Hammouch:** Conceptualization, Writing - original draft, Investigation. **Kottakkaran Sooppy Nisar:** Writing - original draft, Formal analysis, Writing - review & editing.

Declaration of Competing Interest

The authors declare that they have no known competing financial interests or personal relationships that could have appeared to influence the work reported in this paper.

References

[1] Is the World Ready for the Coronavirus?. Editorial. The New York Times. 29 January 2020. Archived from the original on 30 January 2020.
[2] China virus death toll rises to 41, more than 1,300 infected worldwide. CNBC. 24 January 2020. Archived from the original on 26 January 2020. Retrieved 26 January 2020. Retrieved 30 January 2020.
[3] Wuhan, China Population 1950-2020, https://www.macrotrends.net/cities/20712/wuhan/population.
[4] Singh CS, Singh H, Singh VK, Singh OP. Fractional order operational matrix methods for fractional singular integro-differential equation. Appl Math Model 2016;40(23–24):10705–18. https://doi.org/10.1016/j.apm.2016.08.011.
[5] Singh H, Srivastava HM. Jacobi collocation method for the approximate solution of some fractional-order Riccati differential equations with variable coefficients. Physica A 2019;523:1130–49. https://doi.org/10.1016/j.physa:2019.04.120.
[6] Singh CS, Singh H, Singh S, Kumar D. An efficient computational method for solving system of nonlinear generalized Abel integral equations arising in astrophysics. Physica A 2019;525:1440–8. https://doi.org/10.1016/j.physa:2019.03.085.
[7] Singh H, Pandey RK, Baleanu D. Stable numerical approach for fractional delay differential equations. Few-Body Syst 2017;58(6). https://doi.org/10.1007/s00601-017-1319-x.
[8] Singh H, Singh CS. Stable numerical solutions of fractional partial differential equations using Legendre scaling functions operational matrix. Ain Shams Eng J 2018;9(4):717–25. https://doi.org/10.1016/j.asej.2016.03.013.
[9] Singh H, Sahoo MR, Singh OP. Numerical method based on Galerkin approximation for the fractional advection-dispersion equation. Int J Appl Comput Math 2017;3(3):2171–87. https://doi.org/10.1007/s40819-016-0233-0.
[10] Singh H, Srivastava HM, Kumar D. A reliable numerical algorithm for the fractional vibration equation. Chaos Solitons Fractals 2017;103:131–8. https://doi.org/10.1016/j.chaos.2017.05.042.
[11] Singh H, Pandey RK, Singh J, Tripathi MP. A reliable numerical algorithm for fractional advection–dispersion equation arising in contaminant transport through porous media. Physica A 2019;527:121077. https://doi.org/10.1016/j.physa:2019.121077.
[12] Singh H. A new stable algorithm for fractional Navier–stokes equation in polar coordinate. Int J Appl Comput Math 2017;3(4):3705–22. https://doi.org/10.1007/s40819-017-0323-7.
[13] Singh H, Akhavan Ghassabzadeh F, Tohidi E, Cattani C. Legendre spectral method for the fractional Bratu problem. Math Meth Appl Sci 2020;43(9):5941–52. https://doi.org/10.1002/mma.6334.
[14] Kilbas AA, Srivastava HM, Trujillo JJ. Theory and Applications of Fractional Differential Equations, North-Holland Mathematical Studies, Vol. 204. Amsterdam: Elsevier (North-Holland) Science Publishers; 2006.
[15] Khan MA, Atangana A. Modeling the dynamics of novel coronavirus (2019-nCov) with fractional derivative. Alexandria Eng J 2020;59(4):2379–89. https://doi.org/10.1016/j.aej.2020.02.033.
[16] Shah K, Khan ZA, Ali A, Amin R, Khan H, Khan A. Haar wavelet collocation approach for the solution of fractional order COVID-19 model using Caputo derivative. Alexandria Eng J 2020;59(5):3221–31. https://doi.org/10.1016/j.aej.2020.08.028.
[17] Sher M, Shah K, Khan ZA, Khan H, Khan A. Computational and theoretical modeling of the transmission dynamics of novel COVID-19 under Mittag-Leffler Power Law. Alexandria Eng J 2020;59(5):3133–47. https://doi.org/10.1016/j.aej.2020.07.014.
[18] Gomez-Aguilar JF, C-Fraga T, Abdeljawad T, Khan A, Khan H. Analysis of fractal-fractional malaria transmission model. Fractals 2020 Oct 7:2040041.
[19] Khan A, Abdeljawad T, Gómez-Aguilar JF, Khan H. Dynamical study of fractional order mutualism parasitism food web module. Chaos Solitons Fractals 2020;134:109685. https://doi.org/10.1016/j.chaos.2020.109685.
[20] Khan A, Gómez-Aguilar JF, Saeed Khan T, Khan H. Stability analysis and numerical solutions of fractional order HIV/AIDS model. Chaos Solitons Fractals 2019;122:119–28. https://doi.org/10.1016/j.chaos.2019.03.022.
[21] Mahmoud GM, Ahmed M, Alsbagh T. Active control technique of fractional-order chaotic complex systems. Eur Phys J Plus 2016;131:200.
[22] Mahmoud GM, Arafa AA, Abed-Elhameed TM, Mahmoud EE. Chaos control of integer and fractional orders of chaotic Burke-Shaw system using time delayed feedback control. Chaos Solitons Fractals 2017;104:680–92.
[23] Singh H, Srivastava HM. Numerical simulation for fractional-order Bloch equation arising in nuclear magnetic resonance by using the Jacobi polynomials. Appl Sci 2020;10(8):2850.
[24] Atangana A, Qureshi S. Mathematical modeling of an autonomous nonlinear dynamical system for malaria transmission using caputo derivative, fractional order analysis: theory. Methods Applications 2020:225–52.
[25] Owolabi KM, Atangana A. Mathematical modelling and analysis of fractional epidemic models using derivative with exponential kernel. In: Fractional calculus in medical and health science. CRC Press; 2020, pp. 109–128.
[26] Shaikh AS, Shaikh IN, Nisar KS. A mathematical model of COVID-19 using fractional derivative: outbreak in India with dynamics of transmission and control. Adv Differ Equ 2020;2020:373. https://doi.org/10.1186/s13662-020-02834-3.
[27] Petrás I. Modeling and numerical analysis of fractional-order Bloch equations. Comput Math Appl 2011;61:341–56.
[28] Matignon D. Stability results for fractional differential equations with applications to control processing. In: Computational engineering in system application, Lille, France; 1996, pp. 963–968.
[29] Li C-P, Ma Y-T. Fractional dynamical system and its linearization theorem. Nonlinear Dyn 2013;71(4):621–33.

Further reading

[30] Srivastava HM. Fractional-order derivatives and integrals: Introductory overview and recent developments. Kyungpook Math J 2020;60:73–116.
[31] Srivastava HM. Diabetes and its resulting complications: Mathematical modeling via fractional calculus. Public Health Open Access 2020;4(3):1–5. Article ID 2.
[32] Srivastava HM, Saad KM. Numerical simulation of the fractal-fractional Ebola virus. Fractal Fract 2020;4:1–13. Article ID 49.